Photobiomodulation, Photomedicine, and Laser Surgery
Volume 38, Number 6, 2020

Pp. 364–373
DOI: 10.1089/photob.2019.4713

Original Research

Ex Vivo Evaluation of Gingival Ablation with Various Laser Systems and Electroscalpel

Rie Kawamura, DDS,[1] Koji Mizutani, DDS, PhD,[1] Taichen Lin, DDS, PhD,[1–3] Sho Kakizaki, DDS, PhD,[1] Ayako Mimata, PhD,[4] Kowashi Watanabe,[5] Norihito Saito, PhD,[6] Walter Meinzer, DDS,[1] Takanori Iwata, DDS, PhD,[1] Yuichi Izumi, DDS, PhD,[1,7] and Akira Aoki, DDS, PhD[1]

Abstract

Objective: The aim of this study was to perform a systematic and multifaceted comparison of thermal effects during soft tissue ablation with various lasers and an electroscalpel (ES).
Materials and methods: Er:YAG, Er,Cr:YSGG, CO_2, Diode, Nd:YAG lasers (1 W, pulsed or continuous wave), an ES, and a scalpel (Sc; control), were employed for porcine gingival tissue ablation. Temperature changes during ablation were measured by using an infrared thermal imaging camera and a thermocouple. After ablations, the wounds were observed using stereomicroscopy and scanning electron microscopy (SEM), and histological sections were analyzed. Compositional analysis was also performed on ablated sites by SEM wavelength dispersive X-ray spectroscopy.
Results: The surface temperature during irradiation was highest with CO_2 (over 500°C), followed by Diode (267°C) and Nd:YAG (258°C), Er:YAG (164°C), ES (135°C), and Er,Cr:YSGG (85°C). Carbonization was negligible (Er:YAG), slight (Er,Cr:YSGG), moderate (Nd:YAG and ES), and severe (CO_2 and Diode). Under SEM observation, Er:YAG and Er,Cr:YSGG showed smooth surfaces but other devices resulted in rough appearances. Histologically, the coagulated and thermally affected layer was extremely minimal (38 μm in thickness) and free from epithelial collapse for Er:YAG. Compared with other devices, less compositional surface change was detected with Er:YAG and Er,Cr:YSGG; additionally, the use of water spray further minimized thermal influence.
Conclusions: Among various power devices, Er:YAG laser showed the most efficient and refined gingival ablation with minimal thermal influence on the surrounding tissues. Er:YAG and Er,Cr:YSGG lasers with water spray could be considered as minimally invasive power devices for soft tissue surgery.

Keywords: laser, gingiva, ablation, temperature change, thermal coagulation

Introduction

Conventionally, scalpels (Sc) and electroscalpels (ES), have been used for soft tissue surgery in both oral and periodontal surgery. Recently, lasers are also considered to be a good choice for soft tissue management due to effective tissue ablation, hemostatic and bactericidal effects, and relatively clear visual fields during use.[1–8] Moreover, less pain during and after soft tissue ablation is also an advantage of laser application.[9–11]

In general, dental lasers are classified into two groups depending on their specific wavelength; superficially absorbed lasers (Er:YAG, Er,Cr:YSGG, and CO_2 laser) and deeply penetrating lasers (Diode and Nd:YAG laser).[12]

[1]Department of Periodontology, Graduate School of Medical and Dental Sciences, Tokyo Medical and Dental University (TMDU), Tokyo, Japan.
[2]School of Dentistry, Chung Shan Medical University, Taichung, Taiwan.
[3]Department of Dentistry, Chung Shan Medical University Hospital, Taichung, Taiwan.
[4]Research Core, Tokyo Medical and Dental University (TMDU), Tokyo, Japan.
[5]Biomolecular Characterization Unit, Technology Platform Division, RIKEN Center for Sustainable Resource Science, Wako, Japan.
[6]Photonics Control Technology Team, Advanced Photonics Technology Development Group, RIKEN Center for Advanced Photonics, Riken, Wako, Japan.
[7]Oral Care Perio Center, Southern TOHOKU Research Institute for Neuroscience, Southern TOHOKU General Hospital, Koriyama, Japan.

Table 1. Characteristics of Lasers

Laser system	*Wavelength (nm)*	*Power output (W)*	*Irradiation mode*	*Pulse width (μs)*	*Contact tip/probe diameter (μm)*	*ED/PD at tip/probe end*	*Peak power (W)*	*Water spray (+/–)*
Er:YAG	2940	1	Pulsed (50 mJ/20 Hz)	200	600	17.7 J/cm^2/pulse	250	+/–
Er,Cr:YSGG	2780	1	Pulsed (50 mJ/20 Hz)	140	600	17.7 J/cm^2/pulse	357	+/–
CO_2	10,600	1	CW	—	400 (noncontact beam spot)	796.2 W/cm^2 (beam spot)	1	–
Diode	808	1	CW	—	300	1415.4 W/cm^2	1	–
Nd:YAG	1060	1	Pulsed (50 mJ/20 Hz)	100	300	70.8 J/cm^2/pulse	500	–

CW, continuous wave; ED, energy density; PD, power density.

Among superficially absorbed lasers, Er:YAG is widely used in periodontal therapy since it demonstrates effective ablation of both soft and hard tissues because of its high absorption by water.[13,14] Er:YAG laser surgery reportedly showed less thermal damage to surrounding soft tissue[15,16] and faster wound healing compared with electrosurgery.[17] Er,Cr:YSGG shows performance very similar to Er:YAG due to both lasers having very similar wavelengths. CO_2, also superficially absorbed, is often used in soft tissue surgery because of its excellent tissue ablation and strong hemostatic effect.[11,18,19] Diode and Nd:YAG have deeper effects on soft tissues[15,20,21] due to much lower absorption by water.

However, to date, there are no detailed studies systematically comparing various laser systems for thermal effects during soft tissue ablation under the same irradiation conditions. In particular, the detailed differences in soft tissue ablation between Er:YAG and Er,Cr:YSGG have not been clarified. Thus, the aim of this study is to histologically, morphologically, and compositionally investigate thermal effects during gingival soft tissue ablation with various lasers (using equal energy output) and an ES.

Materials and Methods

Sample preparation

Porcine gingiva samples were used as an experimental model for human oral mucosa.[22] Thirty-eight full-thickness porcine keratinized gingiva sheets, $\sim 20 \times 7$ mm each, were prepared from porcine mandibles. Each gingiva sample was fixed at four corners with pins on individual cork boards and stored in a box at high humidity. The 38 samples were distributed as follows: 7 were used for temperature measurement; 24 for optical stereomicroscopy, scanning electron microscopy (SEM), and histology; and the remaining 7 were used for compositional analysis (CA) of the treated surfaces. Five porcine mandibles were also used for temperature measurement of surrounding gingival tissue during treatment.

Laser systems, ES, and Sc (control)

An Sc (#15; Feather Safety Razor Co., Ltd., Gifu, Japan) was used as control. An ES and five kinds of lasers were used as experimental devices: ES [Operer DS-M; J. Morita Mfg. Corp., Kyoto, Japan; Intensity Setting 4.5 (range 0–9), Cutting Mode]; Er:YAG laser [wavelength: 2940 nm, Erwin AdvErl EVO; J. Morita Mfg. Corp.; 1 W, pulsed wave (PW; 20 Hz, actual output 50 mJ/pulse)], Er,Cr:YSGG laser [2780 nm, Waterlase C100; Biolase Technology, Inc., San Clemente, CA; 1 W, PW (20 Hz, 50 mJ/pulse)], CO_2 laser [10,600 nm; Opelaser Pro, Yoshida Dental Mfg. Co., Ltd., Tokyo, Japan; 1 W, continuous wave (CW)], Diode laser (808 nm, S-laser; Showa Yakuhin Kako Co., Ltd., Tokyo, Japan; 1 W, CW), and Nd:YAG laser [1060 nm, formerly manufactured by Mani, Inc., Tochigi, Japan; 1 W, PW (20 Hz, 50 mJ/pulse)] (Table 1). Ablation was performed, generally without water spray, using freehand techniques; perpendicular with no contact (CO_2), oblique contact with light pressure (Er:YAG and Er,Cr:YSGG), or oblique contact with moderate pressure (Diode and Nd:YAG).

Er:YAG and Er,Cr:YSGG laser ablations were also performed with water spray. In addition, Diode and Nd:YAG laser ablations at 1–4 W output were evaluated. For PW lasers using a contact tip, actual energy output was adjusted using a power meter (Field Master and detector LM-P10i; Coherent Company).

Treatment

All gingival cutting/ablations (with Sc, ES, and five lasers) were performed in a linear manner, in a clinically appropriate way to allow sufficient ablation. For each ablation technique, operating times varied by device.

Temperature change measurement

During ablation, an infrared thermal imaging camera (ITIC) (Neo Thermo TVS-700; Nippon Avionics Co., Ltd., Tokyo, Japan) was initially used for temperature measurement. Only

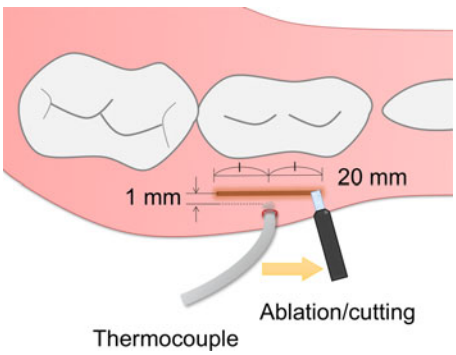

FIG. 1. Graphic of temperature measurement by thermocouple. Porcine mandibles were employed to make 2 cm-long linear cutting/ablations in the mandibular attached gingiva. The thermocouple probe was inserted into the gingiva, midway along, and ~ 1 mm lateral to, the cutting/ablation line.

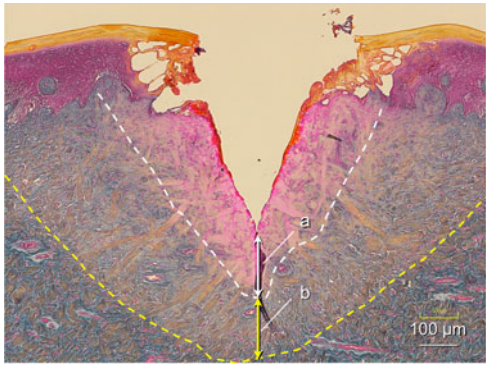

FIG. 2. A representative case of azan slides following gingival tissue ablation/cutting for histometric analysis. Coagulated layer (a) and thermally affected layer (b) around the ablated site were defined as pale pink-colored areas and as grayish pale blue-colored areas, respectively.

one ablation technique was performed (repeated six times) for each of the seven samples. During treatment, thermal images were recorded (rate: 30 images/s) and the maximum temperature point of each thermal image was selected and averaged for each device. Also, temperatures of the surrounding gingiva during ablation were measured using a thermocouple (Digital Thermometer IT-2000; AS ONE Corporation, Osaka, Japan) (Fig. 1). Porcine mandibles, preheated to 36°C simulating the actual human body temperature, were employed at ~26°C room temperature to make 2 cm-long linear cutting/ablations in the mandibular attached gingiva. The thermocouple probe was inserted into the gingiva, midway along, and ~1 mm lateral to, the cutting/ablation line. During ablation, the monitor display was recorded, and the averages of the highest temperatures in the records were calculated.

Morphological analysis

For each sample, a set of all treatments (Sc, ES, five lasers), Er:YAG and Er,Cr:YSGG with water spray treatments, or Diode and Nd:YAG treatments (1, 2, 3, 4 W) were performed. Before any sample preparation, ablation sites on all 24 samples (8 samples for each treatment set) were observed by stereomicroscope (VH-7000; Keyence Corp., NJ). For each set, three specimens for scanning electron microscope (S-4500; Hitachi Ltd., Tokyo, Japan) analysis were obtained from 1/3 sections cut from three of the eight samples. They were fixed with glutaraldehyde, washed overnight in phosphate-buffered saline at 4°C, postfixed with osmium tetroxide at 4°C, and sequentially dehydrated in graded ethanol solutions. Then, the specimens were washed with 3-methyl-butyl-acetate, dried to the critical point, and sputter coated with platinum.

Histological and histometric analyses

For each treatment set, the eight samples were used for histological samples (HS), which were stored in 10% formalin solution, followed by graded ethanol solutions, and then embedded in paraffin. At least eight histological sections, taken at equal intervals, were made from each HS. The sections were stained with either Hematoxylin–Eosin or Azan, and were observed by light microscope. Histometric analysis was then performed on the azan slides. The coagulated layers and thermally affected layers around the ablated sites were defined as pale pink-colored areas and grayish pale blue-colored areas, respectively (Fig. 2). Thickness measurements of coagulated and thermally affected layers at the ablation bottom were performed using software (ImageJ; NIH, Bethesda, MD) by two blinded examiners (K.M. and T.L.).

Compositional analysis

Each of the remaining seven gingiva samples was treated with only one of the seven devices (Sc, ES, five lasers). In the control group, the target connective tissue for CA was prepared by horizontal removal of epithelium with the Sc. The ES and five laser groups had sufficient target connective tissue exposure within the approximately six to eight grooves formed by each device in its respective sample. Each specimen was prepared in the same manner as for SEM. CA for carbon, oxygen, and nitrogen was performed by SEM wavelength dispersive X-ray spectroscopy (SEM-WDS) (JXA-8200 WD/ED Combined Microanalyzer; JEOL Ltd., Tokyo, Japan) at 30 different randomly selected locations for each sample.

Statistical analysis

Data are presented as mean ± standard deviation. Temperature change measurement and CA were analyzed using one-way ANOVA followed by Tukey–Kramer honestly significant difference (HSD) test. Histometric data were analyzed using Steel–Dwass test, or two-way ANOVA and post hoc Tukey–Kramer HSD test for Er:YAG/Er,Cr:YSGG with/without water spray. A p value <0.05 was considered statistically significant.

TABLE 2. IRRADIATION PARAMETERS OF LASERS IN GINGIVAL ABLATION

Laser system	*Power output (W)*	*Exposure duration (sec)*	*Treatment speed (mm/s)*	*Radiant energy (J)*	*Area irradiated (cm^2)*	*Energy fluence (J/cm^2)*
Er:YAG	1	4.4 ± 1.4*,#	1.59 ± 0.39	4.4 ± 1.4	0.047 ± 0.003	95.9 ± 37.1
Er,Cr:YSGG	1	6.8 ± 1.3*	1.00 ± 0.20	6.8 ± 1.3	0.035 ± 0.006	194.0 ± 39.9
CO_2	1	6.4 ± 1.2*	1.06 ± 0.17	6.4 ± 1.2	0.033 ± 0.007	207.0 ± 78.0
Diode	1	10.1 ± 2.8*	0.70 ± 0.22	10.1 ± 2.8	0.046 ± 0.009	226.5 ± 73.3
Nd:YAG	1	26.1 ± 7.1	0.27 ± 0.07	26.1 ± 7.1	0.045 ± 0.008	583.0 ± 136.4

Data represent mean ± SD (n = 10).
Two-way ANOVA and post hoc Tukey–Kramer HSD test.
*,#p < 0.05 compared with Nd:YAG, and Diode, respectively.
HSD, honestly significant difference; SD, standard deviation.

Results

Treatment

The operator-adjusted tip-movement speeds varied greatly among devices according to tissue ablation efficiency: Er:YAG was the fastest followed by CO_2, Sc, Er,Cr:YSGG, Diode, ES, and Nd:YAG (Table 2). Irradiated areas were analyzed and determined from stereomicroscopy images, and the total radiant energy as well as energy fluence were calculated, revealing notable differences in these parameters among lasers (Table 2). For Diode and Nd:YAG, the ablation speeds became faster as the output was raised from 2 to 4 W; 1.46 ± 0.30 mm/s (2 W), 1.87 ± 0.63 mm/s (3 W), 2.20 ± 0.75 mm/s (4 W) for Diode, and 1.05 ± 0.37 mm/s (2 W), 1.12 ± 0.14 mm/s (3 W), and 1.47 ± 0.24 mm/s (4 W) for Nd:YAG.

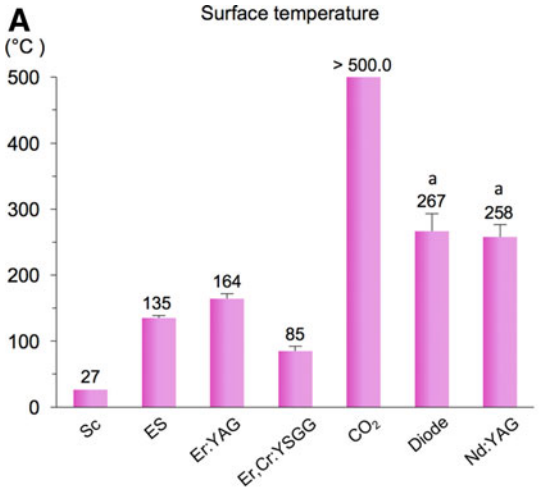

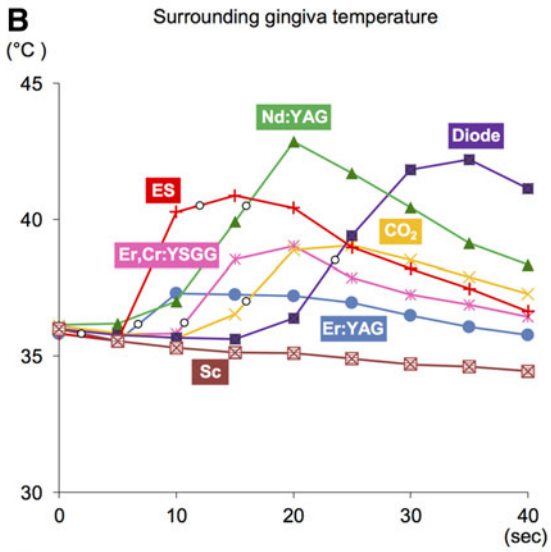

C

Max temperature and temperature rise of surrounding gingiva

Instrument/ device	Max temperature (Mean±SD, °C)	Temperature rise (Mean±SD, °C)
Sc	36.0 ± 0.2	-0.7 ± 0.1
ES	42.7 ± 1.7 *#	7.0 ± 1.9 *#
Er:YAG	38.4 ± 0.4	2.4 ± 0.4
Er,Cr:YSGG	39.3 ± 2.1	3.1 ± 2.1 *
CO_2	39.6 ± 1.4	3.5 ± 1.4 *
Diode	44.1 ± 1.6 *#§†	8.1 ± 1.7 *#§†
Nd:YAG	43.7 ± 2.4 *#§†	7.5 ± 2.6 *#§†

Temperature change measurement

The surface temperature elevation measured by ITIC was maximum for CO_2 (over 500°C), followed by Diode (266.6°C ± 26.6°C), Nd:YAG (257.9°C ± 18.7°C), Er:YAG (164.3°C ± 7.6°C), ES (135.1°C ± 3.7°C), and Er,Cr:YSGG (85.0°C ± 7.4°C). All groups were statistically significantly different with the exception of Diode versus Nd:YAG (Fig. 3A). For Diode, the highest surface temperatures were 266.6°C ± 26.6°C (1 W), 233.3°C ± 23.4°C (2 W), 261.3°C ± 33.5°C (3 W), and 201.3°C ± 20.2°C (4 W), showing no increase. Rather, the temperature at 4 W was significantly decreased than at 1 W ($p < 0.05$).

The temperature of surrounding gingiva was measured by thermocouple (Fig. 3B, C). The pattern of temperature elevation depended on instrument type. The temperature of Diode elevated later compared with other devices (Fig. 3B).

The maximum temperature (temperature change) of surrounding gingiva was 44.1°C ± 1.6°C (8.1°C ± 1.7°C) for Diode, the greatest among all devices. Significantly higher temperature elevations of surrounding gingiva were detected for Diode, Nd:YAG, and ES, compared with the other lasers (Fig. 3C). With water spray, the temperatures (temperature change) for Er:YAG and Er,Cr:YSGG were decreased, 28.0°C ± 0.4°C (−8.1°C ± 0.7°C) and 27.2°C ± 1.5°C (−8.8°C ± 1.4°C), respectively.

FIG. 3. Temperature change during gingival ablation/cutting with various surgical instruments/devices. **(A)** Surface temperature elevation measurement by infrared thermal imaging camera during gingival treatment. The temperature of the ablated tissue surface and/or contact tip/probe during treatment was highest for CO_2, followed by Diode, Nd:YAG, Er:YAG, and ES, and lowest for Er,Cr:YSGG. Data represent mean ± SD ($n = 6$). Significant differences were observed between any two groups, except for between Diode and Nd:YAG groups (indicated by "a"). $p < 0.05$, Tukey–Kramer HSD test. **(B)** Temperature change of surrounding gingiva over time during treatment was measured by thermocouple at ~1 mm away from the middle of the ablation/cutting line. The pattern of temperature elevation depended on instrument type. The temperature with diode was elevated in a delayed manner compared with other devices. Data represent mean ($n = 4$). Small circles: the average time point (during temperature measurement) of the instrument/device's passing by the thermocouple probe. **(C)** Maximum temperature and temperature change of the surrounding gingiva during treatment measured by thermocouple. For Sc, the maximum temperature was read at the beginning and temperature change was read at the finish of incision. Values were highest for Diode, followed by Nd:YAG, ES, CO_2, Er,Cr:YSGG, and lowest for Er:YAG. Data represent mean ± SD ($n = 4$). $^{*,\#,\S,\dagger}p < 0.05$ compared with Sc, Er:YAG, Er,Cr:YSGG, and CO_2, respectively. Tukey–Kramer HSD test. ES, electroscalpel; HSD, honestly significant difference; Sc, scalpel; SD, standard deviation.

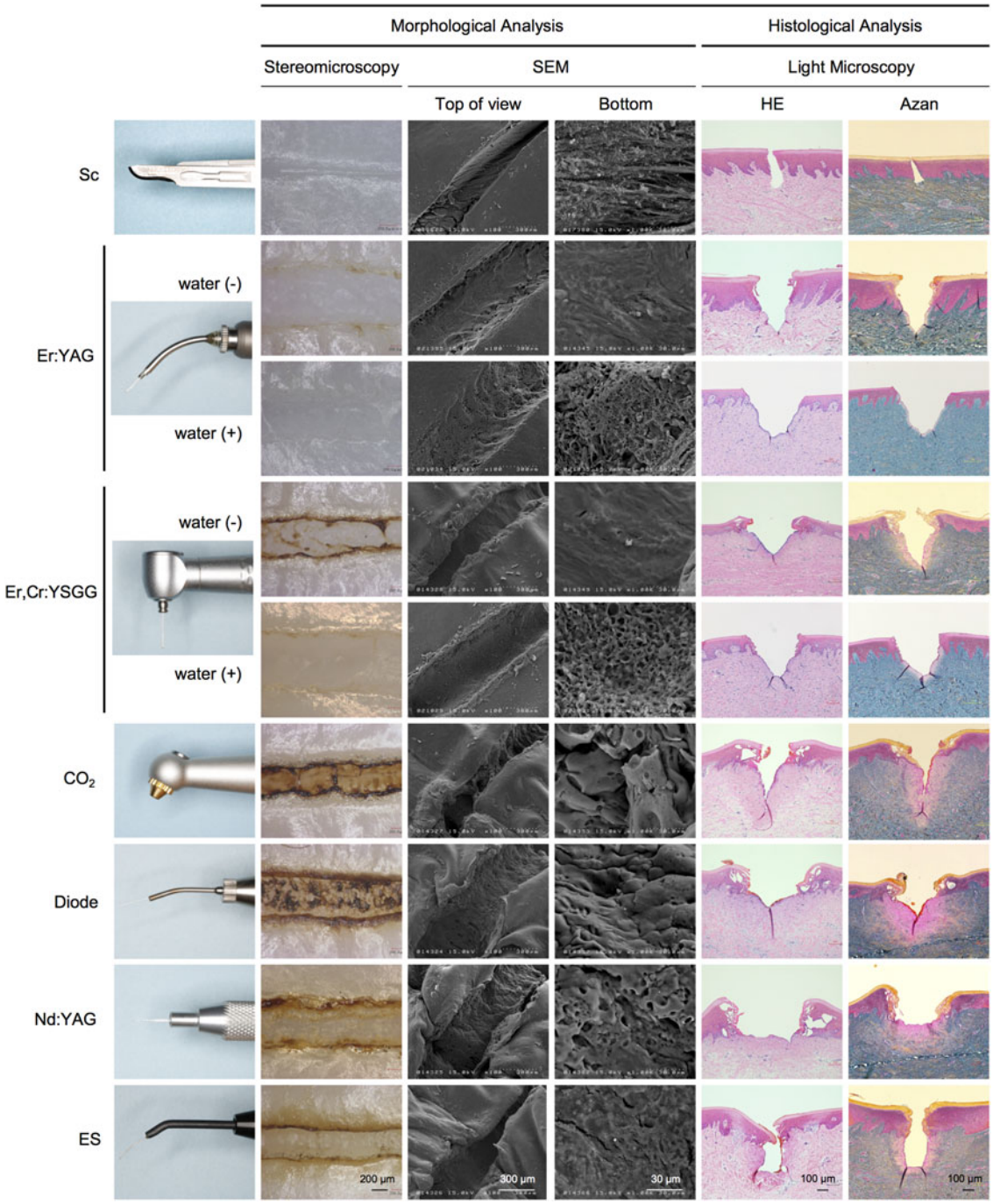

FIG. 4. Stereomicroscopy, SEM, and histological analysis following gingival tissue ablation/cutting with various surgical instruments/devices. Stereomicroscopically, carbonization of the groove edge and bottom was negligible after Er:YAG, slight after Er,Cr:YSGG, moderate after Nd:YAG and ES, and severe for CO_2 and Diode. SEM demonstrated that Sc and Er:YAG/Er,Cr:YSGG with water spray showed fibrous microstructured surface, whereas the Er:YAG and Er,Cr:YSGG without water spray groups resulted in uniformly melted smooth wound surfaces, and the ES, CO_2, Diode, and Nd:YAG groups resulted in melted and resolidified surface appearances. Histologically, the epithelial wound edges were smooth for Er:YAG, Er:YAG/Er,Cr:YSGG with water spray, and Sc, whereas epithelial collapse was observed with other lasers and ES. Thickness of coagulated layer (pale pink-colored areas) was extremely minimal for Er:YAG and Er:YAG/Er,Cr:YSGG with water; however, large coagulation zones were observed for other lasers and ES. Thermally affected layer (grayish pale blue-colored areas) around the coagulation was not detected in Er:YAG, and the thickness was minimally observed for Er,Cr:YSGG, followed by other devices. Use of water spray further reduced thermal changes for Er:YAG and Er,Cr:YSGG. HE, Hematoxylin–Eosin staining; SEM, scanning electron microscopy.

TABLE 3. HISTOMETRIC ANALYSIS FOLLOWING GINGIVAL TISSUE ABLATION/CUTTING WITH VARIOUS SURGICAL INSTRUMENTS/DEVICES

Instrument/ device	*Coagulated layer (μm)*	*Thermally affected layer (μm)*	*Coagulated plus thermally affected layer (μm)*
Sc	0	0	0
ES	82.0 ± 26.2*	94.2 ± 30.1*	176.2 ± 55.2*
Er:YAG	37.7 ± 9.6	0	37.7 ± 9.6
Er,Cr:YSGG	50.6 ± 5.7#	65.7 ± 27.6*	116.4 ± 31.7*
CO_2	163.0 ± 48.8*,#,§	73.6 ± 23.4*	236.6 ± 50.2*,§
Diode	137.9 ± 19.5*,#,§	123.1 ± 33.1*	261.0 ± 45.1*,§
Nd:YAG	137.8 ± 16.3*,#,§	161.8 ± 41.2*,#,§,†	299.6 ± 49.6*,#,§

Data represent mean ± SD ($n = 8$)
*,#,§,† $p < 0.05$ compared with Er:YAG, ES, Er,Cr:YSGG, and CO_2, respectively. Steel–Dwass test.
ES, electroscalpel; Sc, scalpel.

Morphological analysis

Stereomicroscopically, carbonization of the groove edge and bottom was negligible after Er:YAG, slight after Er,Cr:YSGG, moderate after Nd:YAG and ES, and severe after CO_2 and Diode (Fig. 4).

Under SEM observation, Sc and Er:YAG/Er,Cr:YSGG with water spray showed fibrous microstructured ablation bottoms, whereas the Er:YAG and Er,Cr:YSGG without water resulted in uniformly melted smooth wound surfaces, and the ES, CO_2, Diode, and Nd:YAG groups resulted in melted and resolidified surface appearances. The CO_2 laser-treated surface presented coral structures with numerous microcracks and holes. The Diode laser group showed a rocklike or dry soil-like appearance with some microcracks and microdepression. The Nd:YAG laser group presented a magma-like structure and more microholes were observed on the superficial surface, compared with CO_2 and Diode lasers. For Diode, the carbonization tended to be weaker at 2, 3, and 4 W than at 1 W (Fig. 5).

Histological and histometric analyses

The grooves with Sc, ES, Er:YAG, Er,Cr:YSGG, CO_2, were sharp and deep, but with Diode and Nd:YAG, the grooves were flatter and did not deeply ablate connective tissue at 1 W (Fig. 4). However, with these lasers, ablation depth increased according to the elevation of output (Fig. 5). The epithelial wound edges were smooth for Sc, Er:YAG, and Er:YAG/Er,Cr:YSGG with water spray, whereas epithelial collapse was observed with Er,Cr:YSGG, other lasers, and ES.

TABLE 4. HISTOMETRIC ANALYSIS FOLLOWING GINGIVAL TISSUE ABLATION FOR ERBIUM LASERS WITH/WITHOUT USE OF WATER SPRAY

Erbium laser	*Water spray (+/–)*	*Coagulated layer (μm)*	*Thermally affected layer (μm)*	*Coagulated plus thermally affected layer (μm)*
Er:YAG	–	37.7 ± 9.6	0	37.7 ± 9.6§
	+	17.9 ± 2.1*	0	17.9 ± 2.1§
Er,Cr:YSGG	–	50.6 ± 5.7*,#	65.7 ± 27.6	116.4 ± 31.7
	+	33.1 ± 1.4#,§	0	33.1 ± 1.4§

Data represent mean ± SD ($n = 8$).
*,#,§ $p < 0.05$ compared with Er:YAG (–), Er:YAG (+), and Er,Cr:YSGG (–), respectively. Two-way ANOVA and post hoc Tukey–Kramer HSD test.

Thickness of coagulated layer was minimal for Er:YAG (37.7 ± 9.6 μm) followed by Er,Cr:YSGG (50.6 ± 5.7 μm), and ES (82.0 ± 26.2 μm). Moreover, the above coagulated layers were significantly thinner compared with other laser groups. Thermally affected layer around the coagulation was not detected for Er:YAG, and the thickness was minimally observed in Er,Cr:YSGG (65.7 ± 27.6 μm), followed by CO_2, ES, Diode, and Nd:YAG. The total width of coagulated and thermally affected layer was minimal (37.7 ± 9.6 μm) for Er:YAG and was significantly thinner as compared with Er,Cr:YSGG (116.4 ± 31.7 μm), ES, CO_2, Diode, and Nd:YAG (Table 3). With the use of water spray, coagulation was significantly reduced for Er:YAG (17.9 ± 2.1 μm) and for Er,Cr:YSGG (33.1 ± 1.4 μm), and thermally affected layer was none for both lasers. The total width was also reduced for Er:YAG (17.9 ± 2.1 μm) and Er,Cr:YSGG (33.1 ± 1.4 μm), with water spray (Table 4).

For both Diode and Nd:YAG, the total thickness of coagulated and thermally affected layer was not significantly different regardless of the energy output (Supplementary Table S1).

Compositional analysis

Carbon slightly but significantly decreased in all treatment groups and oxygen was most significantly increased with CO_2, followed by Diode, Nd:YAG, Er,Cr:YSGG, ES, and Er:YAG. Nitrogen was most significantly decreased for CO_2, followed by other devices, except for Er:YAG, compared with control (Sc). In total, the largest differences were seen with CO_2 followed by Diode and Nd:YAG. Interestingly, Er:YAG, ES, and Er,Cr:YSGG showed less change, compared with other lasers, and the Er:YAG-treated surface was closest to the control surface (Fig. 6).

Discussion

Er:YAG, Er,Cr:YSGG, and CO_2 lasers were able to ablate soft tissue readily at 1 W output; however, such soft tissue ablation at 1 W was not feasible with Diode and Nd:YAG. An output over 2–5 W is reportedly appropriate for oral soft tissue ablation with Nd:YAG.[23,24] In the present study, indeed, ablation speed for Diode and Nd:YAG increased as power output increased.

The surface temperature elevations were the highest (over 500°C) with CO_2. Although ITIC measured temperatures of not only the tissue surface but also the contact tip/probe during contact ablation, in the case of noncontact CO_2 the tissue surface temperature during thermal evaporation caused by laser–tissue interaction was more validly determined. Still, the exact highest temperature with CO_2 was not detected because it exceeded the measurable temperature range of the camera.

Stereomicroscopically, CW lasers (CO_2 and Diode) showed severe black-colored carbonization of treated groove edges and/or bottoms, possibly due to high surface temperature elevations (over 500°C and 267°C, respectively). Coagulated layer was thickest for CO_2; interestingly however, the total

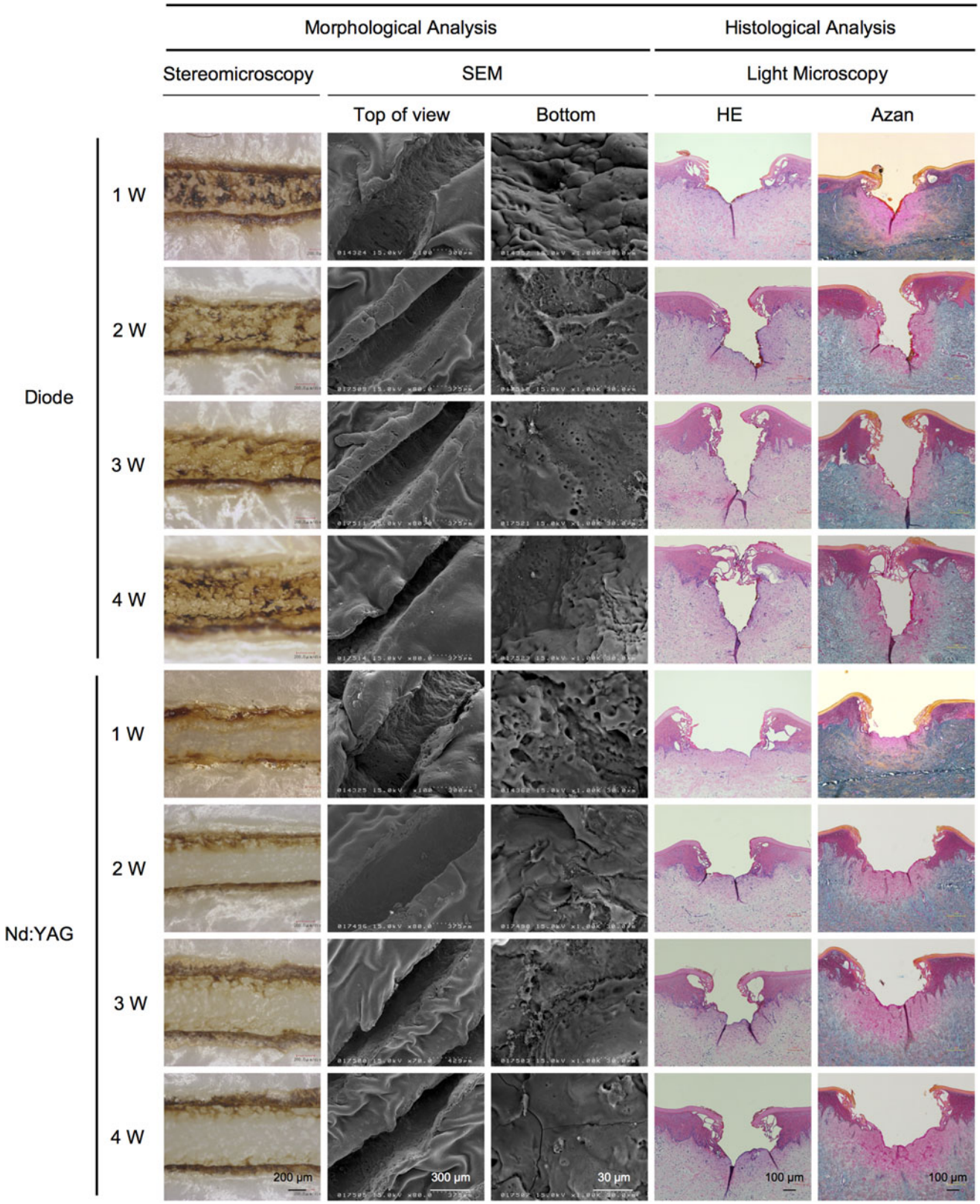

FIG. 5. Stereomicroscopy, SEM, and histological analysis after gingival tissue ablation with Diode and Nd:YAG at 1, 2, 3, and 4 W output. With both Diode and Nd:YAG, ablation depth increased with output elevation, whereas thickness of coagulated layer (pale pink-colored areas) and thermally affected layer (grayish pale blue-colored areas) around the coagulation were not significantly different regardless of the energy output.

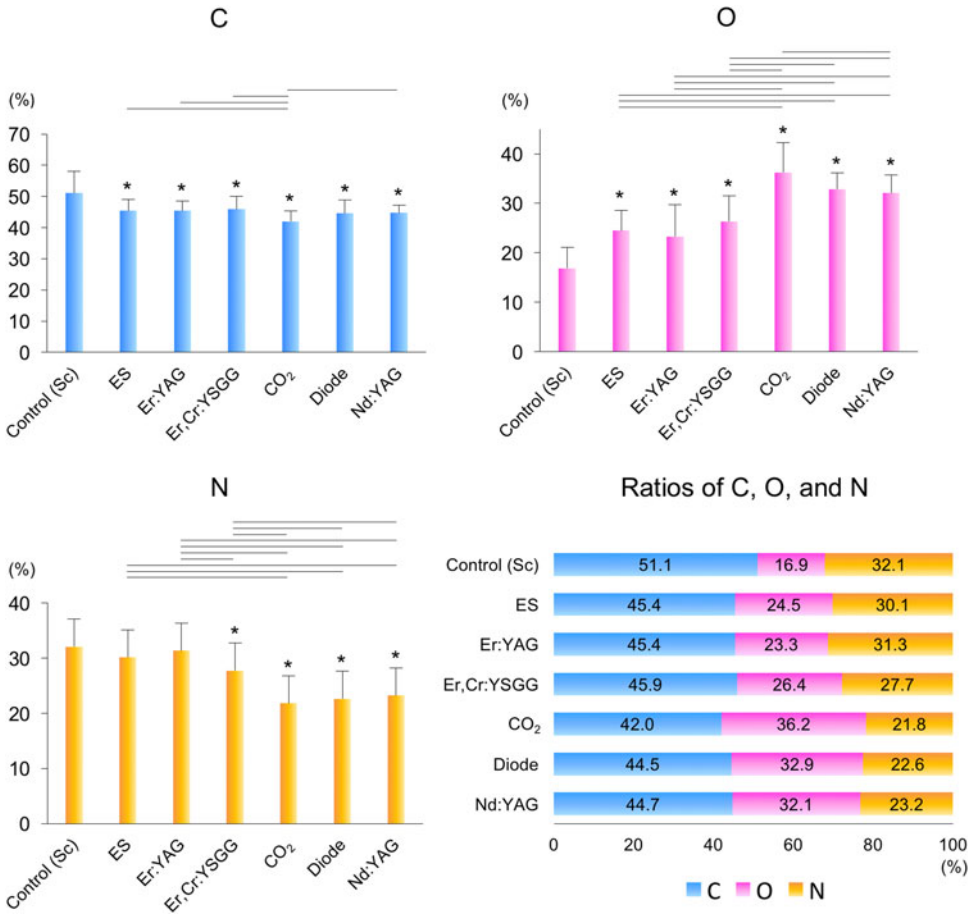

FIG. 6. Compositional analysis following gingival tissue ablation/cutting with various surgical instruments/devices. The percentage of each element (Carbon: C, Oxygen: O, Nitrogen: N, 100% in total) for each device is presented. Carbon significantly decreased in all treatment groups and oxygen was most significantly increased with CO_2, followed by Diode, Nd:YAG, and other devices. Nitrogen was most significantly decreased for CO_2, followed by Diode, Nd:YAG, and Er,Cr:YSGG compared with control (Sc). In total, the largest differences were seen with CO_2 followed by Diode and Nd:YAG. Interestingly, Er:YAG, ES, and Er,Cr:YSGG showed less change and the Er:YAG-treated surface was compositionally closest to the control surface. Data represent mean ± SD ($n = 30$). *$p < 0.05$ compared with control. The bars indicate significances between two groups. Tukey–Kramer HSD test.

zone of coagulated plus thermally affected layer was thicker with Diode and Nd:YAG than with CO_2. This is because CO_2 laser is of the superficially absorbed type, with momentarily generated heat during thermal evaporation occurring in and limited to, the superficial layer, not spreading and reaching the deeper tissues.

Histologically, the coagulated layer showed that collagen fiber structure disappeared and became amorphous, similar to observations with denatured collagen in burn wounds.[25] Although in the thermally affected layer fiber structure still remained, the structure was somewhat altered, and the dyeability of Azan, specific for collagen fiber, was a little lower than in the surrounding intact tissue. This may be due to the thermal influence of the lasers and ES, inducing denaturation of collagen proteins in the surrounding tissue.

Tissue ablation effects of lasers are influenced by various characteristics, such as wavelength, output, pulse width/peak power (beam intensity), and irradiation procedures such as treatment speed. In general, the shorter the pulse width, the greater is the peak power and the less is the thermal effect. However, in this study, no significant association was observed between pulse width/peak power and tissue ablation/thermal influences. This was because the differences in wavelengths and treatment speeds were primarily responsible for the different results of tissue ablation and thermogenesis in the present study. Regarding energy fluence, it showed tendencies for positive association with histological thermal changes; however, the findings were not found to be significant (data not shown).

Nd:YAG and Diode showed a similar tendency in histological changes (coagulated and thermally affected layer) as well as surface temperature elevation, whereas carbonization in the bottom of the groove was generally less and moderate with Nd:YAG, compared with severe carbonization caused by Diode. This might be due to the property of pulsed Nd:YAG lasers having high peak power, unlike CW Diode, and due to differences in heat generation efficiency in the tips. For these lasers, part of the emitting light is converted into heat by refraction or diffused reflection at the tip end, creating a condition called hot tip. Accordingly, the tissue was vaporized and coagulated as a result of contact with the highly heated tip, by secondary thermal effects rather than by the laser energy itself.[1] Thus, the detected surface temperature seemed to indicate the temperature of hot tips. Of note, compared with Nd:YAG, the temperature elevation of surrounding tissue with Diode showed a slowly rising pattern and occurred later after ablation (Fig. 3B), suggesting that heat generated on the ablated surface was more gradually conducted to the surrounding tissue with Diode. However, the precise mechanism is unknown and further investigation is required to clarify these phenomena with Nd:YAG and Diode.

Meanwhile, the temperature elevation detected with Er,Cr:YSGG was the lowest (85.0°C). This was because Er,Cr:YSGG laser's contact tip is composed of sapphire, which allows high transmittance of light at the wavelength range of ~ 0.2–$5.5\ \mu$m,[26] resulting in less thermogenesis

during irradiation. In contrast, Er:YAG laser employed a quartz curved-type tip, which absorbs its wavelength to some extent, creating some heat. Therefore, compared with Er,Cr:YSGG, higher temperature elevation (164°C) occurred during ablation with Er:YAG due to the thermogenesis of the tip itself during irradiation.

Interestingly, despite those findings, histological analysis demonstrated lower thermal influences with Er:YAG as compared with Er,Cr:YSGG. Following Er:YAG, almost no carbonization was observed, and both SEM and histological observation showed a smooth ablation surface. In addition, histologically, the coagulated and thermally affected layer was thinnest for Er:YAG. These findings indicate that Er:YAG laser energy was more directly and efficiently consumed for tissue ablation, allowing for less thermal influence than Er,Cr:YSGG. Thus, Er:YAG may be the least invasive device for soft tissue ablation among powered surgical devices. Further, with the addition of water spray, both Er:YAG and Er,Cr:YSGG, would be less invasive devices as evidenced by comparable minimal thermal influences on surrounding tissues.

CA of laser-irradiated soft tissue surfaces was performed for the first time in the present study and subsequently, when the CA results were combined with the results of coagulation width measurement, it was found that the larger the thermal influence, the more oxidized the irradiated surface became. Compositionally, the Er:YAG laser-treated surface most closely resembled the control surface.

This study revealed that the surface temperature during irradiation was considerably high, in particular for CO_2, Diode, and Nd:YAG lasers. Thus, to improve clinical safety with these lasers, it is necessary to move the handpiece constantly to avoid heat accumulation in the tissues. Also, attention should be paid to avoid accidental irradiation of, and contact with, the surrounding tissues. Regarding the thermal influence on bone tissue, previous reports showed that osteonecrosis occurred above 47°C.[27] Since, in the present study, the temperature of the tissue 1 mm away from the ablation site was 44°C at most (for Diode), thermal influence to the periosteum and bone tissue could be minimized if an appropriate distance is maintained. However, substantial thermal influences reach a distance of $\sim$230–300 μm with CO_2, Diode, and Nd:YAG. Thus, with these lasers, sufficient care must be taken during irradiation of tissues close to bone. In the case of erbium lasers, since thermal influences are effectively minimized to begin with (with even less thermogenesis when accompanied by water spray), clinical safety is highly attainable in general.

Conclusions

Among various laser systems and ES, Er:YAG showed the most efficient and refined gingival ablation with minimal thermal influence on the surrounding tissues as well as less compositional surface change. Er:YAG as well as Er:YAG/Er,Cr:YSGG with water spray could serve as minimally invasive power devices for soft tissue surgery. In contrast, other lasers and ES, with relatively large thermal effects, would nonetheless have advantageous hemostatic effects. Therefore, it is important with soft tissue surgery to choose the most appropriate device and parameters according to the purpose and demands of the particular surgery, and the operator's skills.

Acknowledgments

The authors would like to extend their appreciation to J. Morita Mfg. Corp., Showa Yakuhin-kako Co., Ltd., Yoshida Dental Mfg. Co., Ltd., Wavelength Corp., and Mani, Inc., in Japan for their kind help, to Mrs. Shingo Iwamoto and Haruhiko Murakami, J. Morita Mfg. Corp. and Drs. Yoshiyuki Sasaki and Kazuki Watanabe of TMDU, and to the staff at TMDUs Research Core for their valued assistance.

Author Disclosure Statement

No competing financial interests exist.

Funding Information

This work was supported by the Japan Society for the Promotion of Science KAKENHI (16K11825 to Akira Aoki).

Supplementary Material

Supplementary Table S1

References

1. Aoki A, Mizutani K, Schwarz F, et al. Periodontal and peri-implant wound healing following laser therapy. Periodontol 2000 2015;68:217–269.
2. Research Science and Therapy Committee of the American Academy of Periodontology. Lasers in periodontics. J Periodontol 2002;73:1231–1239.
3. Pick RM, Colvard MD. Current status of lasers in soft tissue dental surgery. J Periodontol 1993;64:589–602.
4. Rossmann JA, Cobb CM. Lasers in periodontal therapy. Periodontol 2000 1995;9:150–164.
5. Mizutani K, Aoki A, Coluzzi D, et al. Lasers in minimally invasive periodontal and peri-implant therapy. Periodontol 2000 2016;71:185–212.
6. Pang P, Andreina S, Aoki A, et al. Laser energy in oral soft tissue applications. J Laser Dent 2010;18:123–131.
7. Tamarit-Borrás M, Delgado-Molina E, Berini-Aytés L, Gay-Escoda C. Removal of hyperplastic lesions of the oral cavity. A retrospective study of 128 cases. Med Oral Patol Oral Cir Bucal 2005;10:151–162.
8. Ortega-Concepción D, Cano-Durán JA, Peña-Cardelles JF, Paredes-Rodríguez VM, González-Serrano J, López-Quiles J. The application of diode laser in the treatment of oral soft tissues lesions. A literature review. J Clin Exp Dent 2017;9: e925–e928.
9. López-Jornet P, Camacho-Alonso F. Comparison of pain and swelling after removal of oral leukoplakia with CO_2 laser and cold knife: a randomized clinical trial. Med Oral Patol Oral Cir Bucal 2013;18:e38–e44.
10. Hall RR, Hill DW, Beach AD. A carbon dioxide surgical laser. Ann R Coll Surg Engl 1971;48:181–188.
11. Tuncer I, Ozçakir-Tomruk C, Sencift K, Cöloğlu S. Comparison of conventional surgery and CO_2 laser on intraoral soft tissue pathologies and evaluation of the collateral thermal damage. Photomed Laser Surg 2010;28: 75–79.
12. Aoki A, Sasaki KM, Watanabe H, Ishikawa I. Lasers in nonsurgical periodontal therapy. Periodontol 2000 2004;36:59–97.

13. Ishikawa I, Aoki A, Takasaki AA. Potential applications of Erbium:YAG laser in periodontics. J Periodontal Res 2004; 39:275–285.
14. Walsh LJ. The current status of laser applications in dentistry. Aust Dent J 2003;48:146–155; quiz 198.
15. Merigo E, Clini F, Fornaini C, et al. Laser-assisted surgery with different wavelengths: a preliminary ex vivo study on thermal increase and histological evaluation. Lasers Med Sci 2013;28:497–504.
16. Romeo U, Libotte F, Palaia G, et al. Histological in vitro evaluation of the effects of Er:YAG laser on oral soft tissues. Lasers Med Sci 2012;27:749–753.
17. Sawabe M, Aoki A, Komaki M, Iwasaki K, Ogita M, Izumi Y. Gingival tissue healing following Er:YAG laser ablation compared to electrosurgery in rats. Lasers Med Sci 2015; 30:875–883.
18. Karimi A, Sobouti F, Torabi S, et al. Comparison of carbon dioxide laser with surgical blade for removal of epulis fissuratum. A randomized clinical trial. J Lasers Med Sci 2016;7:201–204.
19. Monteiro LS, Mouzinho J, Azevedo A, Câmara MI, Martins MA, La Fuente JM. Treatment of epulis fissuratum with carbon dioxide laser in a patient with antithrombotic medication. Braz Dent J 2012;23:77–81.
20. Cercadillo-Ibarguren I, España-Tost A, Arnabat-Domínguez J, Valmaseda-Castellón E, Berini-Aytés L, Gay-Escoda C. Histologic evaluation of thermal damage produced on soft tissues by CO_2, Er,Cr:YSGG and diode lasers. Med Oral Patol Oral Cir Bucal 2010;15:e912–e918.
21. Azevedo AS, Monteiro LS, Ferreira F, et al. histological evaluation of the surgical margins made by different laser wavelengths in tongue tissues. J Clin Exp Dent 2016;8: e388–e396.
22. Wong JW, Gallant-Behm C, Wiebe C, et al. Wound healing in oral mucosa results in reduced scar formation as compared with skin: evidence from the red Duroc pig model and humans. Wound Repair Regen 2009;17:717–729.
23. Perry DA, Goodis HE, White JM. In vitro study of the effects of Nd:YAG laser probe parameters on bovine oral soft tissue excision. Lasers Surg Med 1997;20:39–46.
24. Parker S. Lasers and soft tissue: 'loose' soft tissue surgery. Br Dent J 2007;202:185.
25. Jabeen S, Clough ECS, Thomlinson AM, Chadwick SL, Ferguson MWJ, Shah M. Partial thickness wound: does mechanism of injury influence healing? Burns 2019;45:531–542.
26. John AJ. Infrared physics and engineering. New York: McGraw-Hill, 1963; pp. 222–223.
27. Eriksson AR, Albrektsson T. Temperature threshold levels for heat-induced bone tissue injury: a vital-microscopic study in the rabbit. J Prosthet Dent 1983;50:101–107.

Address correspondence to:
Akira Aoki, DDS, PhD
Photoperiodontics
Department of Periodontology
Graduate School of Medical and Dental Sciences
Tokyo Medical and Dental University (TMDU)
1-5-45 Yushima, Bunkyo-ku
Tokyo 113-8549
Japan

E-mail: aoperi@tmd.ac.jp

Received: June 18, 2019.
Accepted after revision: October 1, 2019.
Published online: March 11, 2020.